# Recent Results of High $p_T$ Physics at the CDF II

Soushi Tsuno (CDF Collaboration)
Department of Physics, Faculty of Science, Okayama University
3-1-1 Tsushima-naka, Okayama 700-8530, Japan

**Abstract**

The Tevatron Run II program is in progress since 2001. The CDF experiment have accumulated roughly five times more data than in Run I, with much improved detectors. Preliminary results from the CDF experiment are presented. We focus on the recent high $p_T$ physics results in Tevatron Run II program.



## 1 Introduction

The CDF (Collier Detector at Fermilab) experiment is a general purpose experiment for the studies of $p\bar{p}$ collisions at the Tevatron Collider located at the Fermi National Accelerator Laboratory (Fermilab), in Batavia, Illinois, U.S.. The Tevatron accelerator is the highest-energy proton-antiproton accelerator machine in the world. The Tevatron accelerator [1] and the CDF(D0) [2] detectors have upgraded since the termination of Run I experiment in 1996.

The accelerator complex had added the Main Injector, replacing the old Main Ring, to inject higher intensity beams to the Tevatron and to produce more anti-protons to be used for collision. The Tevatron beam energy has been increased and it resulted in a center-of-mass energy of 1.96 TeV in Run II from 1.8 TeV in Run I. The instantaneous luminosity has improved steadily since the beginning of Run II, and is marking with a new record. The record value at this conference was $6.3 \times 10^{31}$ cm$^{-2}$s$^{-1}$ which was about 3 times higher than the Run-I record value and is close to the Run-IIa goal of $8.6 \times 10^{31}$. The integrated luminosity delivered to each experiment has exceeded 450 pb$^{-1}$, and with about 80% of them recorded by the detector. The CDF detector has undergone the upgrade of a completely new tracking and forward calorimetry systems, a extension of muon tracking, and lots of minor changes as well as DAQ upgrades.

Since the Tevatron Run-II program has officially started in March 2001, the CDF is extensively exploring a new physics beyond Standard Model. Measuring the high $p_T$ phenomena to establish the SM in electroweak sector is also important in that it may give us a knowledge in nature about symmetry breaking. In this paper, we describe our recent results for the high $p_T$ physics.

## 2 Electroweak Physics

### 2.1 Production of single gauge bosons

Since the great success of the Standard Model in the recent decades, there has been no doubt that the gauge theories are capable to describe the interactions between elementary particles. With larger colliding energy available to probe higher energy scattering events, a high precision measurement may open a beautiful structure among them.

The CDF has performed studies of various aspects of the weak boson properties. They are cleanly identified with their decays to leptons (mostly electrons or muons). The leptonicaly decaying Z boson is identified by using two clean high $p_T$ lepton candidates within the mass range of Z boson. The invariant mass distribution for Z boson candidates is shown in Figure 1. The production cross sections are measured to be [3]

$$\sigma(p\bar{p} \to Z/\gamma^* \to l^+l^- + X) = 254.3 \pm 3.3(stat.) \pm 4.3(syst.) \pm 15.3(lumi.) \quad \text{pb},$$

in good agreement with a theory prediction of 251.3 ± 5.0 pb at NNLO level with MRST [4].

Decays of W bosons are distinguished by one high $p_T$ lepton and missing transverse energy from undetectable neutrino. The transverse mass distribution for W boson candidates is shown in Figure 2, where the transverse mass is given as $M_T = \sqrt{2E_T^l E_T^{missing}[1 - \cos(\Delta\phi^{l-missing})]}$. The production cross

sections are measured to be [3]

$$\sigma(p\bar{p} \to W \to l\nu + X) = 2777 \pm 10(stat.) \pm 52(syst.) \pm 167(lumi.) \quad \text{pb},$$

in good agreement with a theory prediction of 2687 ± 54 pb at NNLO level with MRST [4].

In Figure 3, we summarize the single boson production cross sections as a function of the center-of-mass energy starting from earlier measurement at CERN together with our previous measurements of Run I. We can see a good agreement with the theory predictions.

The ratio of the Z and W boson production cross sections is used as an indirect measurement of the W boson mass and width. The ratio is defined as

$$R \equiv \frac{\sigma(p\bar{p} \to W \to l\nu + X)}{\sigma(p\bar{p} \to Z/\gamma^* \to l^+l^- + X)} = 10.93 \pm 0.15(stat.) \pm 0.13(syst.).$$

Using a theoretical calculation of the ratio of production cross sections and a measured value of the branching ratio of Z boson at LEP experiment [5], we can extract the leptonic branching ratio or total width of W boson,

$$Br.(W \to l\nu) = 0.1089 \pm 0.0022 \quad , \quad \Gamma_W = 2.071 \pm 0.040 \quad \text{GeV}.$$

The current world average for the W boson width is shown in Figure 4.

One of remarkable achievements in CDF II experiment is that the track reconstructions are possible at the trigger level. As a result of this, tau candidate events are able to be triggered, then statistically accessible to study various tau lepton physics. Reconstruction of the tau decay is accomplished by finding an energy cluster in the calorimeter with isolated tracks matched to it. Individual $\pi^0$ particles from the tau decay are reconstructed using detectors in the calorimeter at shower max, and the combined invariant mass of the cluster is required to be less than the mass of the tau. Obtained production cross section of Z and W decaying into tau leptons are [6]

$$\sigma(p\bar{p} \to Z/\gamma^* \to \tau^+\tau^- + X) = 242 \pm 48(stat.) \pm 26(syst.) \pm 15(lumi.) \quad \text{pb},$$
$$\sigma(p\bar{p} \to W \to \tau\nu + X) = 2.62 \pm 0.07(stat.) \pm 0.21(syst.) \pm 0.16(lumi.) \quad \text{nb}.$$

The lepton universality can be measured with three generations of lepton family. Calculating the R ratio for each channel separately, we can derive the ratio of the coupling constants,

$$\frac{g_\mu}{g_e} = 1.011 \pm 0.018 \quad , \quad \frac{g_\tau}{g_e} = 0.99 \pm 0.04.$$

These are all consistent with the SM predictions.

In Z boson production, the forward backward asymmetry yields a measurement of $\sin^2\theta_W$ (mixture with up- and down-type quark in PDF) and a search for higher mass Z' bosons. This is unique tests only at the Tevatron. The asymmetry is defined as

$$A_{fb} \equiv \frac{\sigma(\cos\theta > 0) - \sigma(\cos\theta < 0)}{\sigma(\cos\theta > 0) + \sigma(\cos\theta < 0)},$$

where $\theta$ is the polar angle between the incoming proton and the outgoing lepton. The distributions of the asymmetry around Z-pole and in high mass region are shown in Figure 5 and 6, respectively. Both distributions agree with the SM predictions. Extracting $\sin^2\theta_W$ from those shape, we can obtain [7]

$$\sin^2\theta_W = 0.2238 \pm 0.0046(stat.) \pm 0.0020(syst.).$$

## 2.2 Pair production of gauge bosons

An non-abelian gauge theory describing the electroweak interactions induces the three- and four-point self-couplings of gauge bosons. Measurements of the pair production of the gauge bosons is a fundamental tests for those self-couplings. The cross section for $W^+W^-$ productions has been measured in the *dilepton*

channel at CDF [8]. The azimuthal angle between the missing transverse energy and the closest lepton for it is uesd to enhance the candidate events, which is shown in Figure 7. The measured value is

$$\sigma(p\bar{p} \to W^+W^- \to l^+l^-\nu\bar{\nu} + X) = 14.3^{+5.6}_{-4.9}(stat.) \pm 1.6(syst.) \pm 0.9(lumi.) \quad \text{pb},$$

which is consistent with the SM expectations [9].

Inclusive W$\gamma$ and Z$\gamma$ productions are also studied [10]. The photon can be radiated from the initial state quark and final state lepton in addition to from the W boson with the triple gauge coupling which contribution is presumably enhanced in high $E_T$ region. The $E_T$ spectra probes the anomaly to that triple gauge boson coupling. In Figure 8, we show the photon $E_T$ distribution, and no excess is observed. The measured production cross sections are

$$\sigma(p\bar{p} \to W\gamma + X) \cdot Br.(W \to l\nu) = 19.7 \pm 1.7(stat.) \pm 2.0(syst.) \pm 1.1(lumi.) \quad \text{pb},$$
$$\sigma(p\bar{p} \to Z/\gamma^*\gamma + X) \cdot Br.(Z \to l^+l^-) = 5.3 \pm 0.6(stat.) \pm 0.4(syst.) \pm 0.3(lumi.) \quad \text{pb}.$$

Those results are compared with the NLO calculation [11] of 19.3 ± 1.3 pb for W$\gamma$ production and 5.4 ± 0.4 pb for Z$\gamma$ production, and both results are a good agreement with the theoretical calculation. A more direct test of the gauge couplings can be performed if photon angular distributions of those events are studied and radiation amplitude zero is looked for directly.

# 3 Top Quark Physics

## 3.1 Overview

Since the discovery of the top quark in 1995 by the CDF and D0 collaborations [12], the studies of the top quark properties have been the most important mission in Run II physics program. While the existence of the top quark demonstrates correctness of the Standard Model, nothing tells us about the hierarchy problem of the mass gap among the quark family and generations. Detailed studies of their properties will reveal something about a fundamental nature of the matter.

At Tevatron, the production mechanism is a top and anti-top quarks pair creation via quark-antiquark annihilation (85%) or via gluon fusion (15%). Then, the top quark is assumed to decay into W boson and bottom quark immediately. The final observed signature thus depends on the W bosons decay from top quarks. The analysis strategy is basically categorized by the *dilepton* ($l^+\nu bl^-\bar{\nu}\bar{b}$, ∼7% of all $t\bar{t}$ events), *lepton+jets* ($l\nu bq\bar{q'}\bar{b}$, ∼35%), and *all hadronic* ($qq'bq\bar{q'}\bar{b}$, ∼44%) channels. The analysis is also categorized by the b-tagging algorithms, but combined results are only presented in this section.

## 3.2 Production cross sections

The *dilepton* channel is characterized by two leptons with high transverse momentum and missing energy from the undetected neutrinos and two jets from the b quarks. This channel is relatively clean to the other channels, but statistically limited. To increase the overall acceptance of two leptons, the selection criteria to identify the leptons is loosen, while the tight selection does not suffer from the background contamination. Figure 9 shows the jet multiplicity distribution of the candidate events in case of one tight lepton plus isolated track data set. Those combined result for the production cross section is [13]

$$\sigma(p\bar{p} \to t\bar{t} + X) = 7.0^{+2.4}_{-2.1}(stat.)^{+1.6}_{-1.1}(syst.) \pm 0.4(lumi.) \quad \text{pb},$$

in good agreement with a theory prediction of $6.7^{+0.7}_{-0.9}$ pb at NLO level with assuming the top mass of 175 GeV [14].

The *lepton+jet* channel requires one lepton and 4 more jets in the final state. The sample size is larger than the *dilepton* sample, but there is a significant background contamination from the associated production of W boson with jets. The purity of the sample can be improved by the identification of at least one b-quark jets. We typically use two different b-tagging algorithms. The first one makes used of the long lifetime of the b hadrons to reconstruct a displaced secondary vertex. The second one identifies the soft muon from semileptonic b-decay. The signal to noise ratio can be further improved by requiring the

scalar sum of the energy in the event, $H_T$, to be greater than 200 GeV. The jet multiplicity distribution of these candidate events by the displaced secondary vertex technique with $H_T > 200$ GeV are shown in Figure 10. The excess of events in the bins $N_{jet} \geq 3$ bins is nicely described after the inclusion of top contributions. The production cross sections from both b-tagging algorithms are measured to be [15, 16]

$$\begin{aligned}\sigma(p\bar{p} \to t\bar{t} + X) &= 5.6^{+1.2}_{-1.1}(stat.)^{+0.9}_{-0.6}(syst.) \quad \text{pb} \quad \text{(Secondary Vertex)}, \\ &= 5.2^{+2.9}_{-1.9}(stat.)^{+1.3}_{-1.0}(syst.) \quad \text{pb} \quad \text{(Soft Lepton)}.\end{aligned}$$

Instead of counting signal and background events, one can extract the fraction of $t\bar{t}$ events in the lepton + jets sample by fitting one or more kinematic variables in the data to the expected shapes from signal and backgrounds. As already mentioned, the $H_T$ variable is strong discrimination power of signal to backgrounds. Figure 11 shows the $H_T$ distribution with the expected shapes of signal and backgrounds. At least 4 more jets are required for the fitting to $H_T$ in this plot. The estimated production cross section is [17]

$$\sigma(p\bar{p} \to t\bar{t} + X) = 4.7 \pm 1.6(stat.) \pm 1.8(syst.) \quad \text{pb}.$$

Summary of the measured $t\bar{t}$ cross section from CDF is presented in Figure 12. Note that there are many other measurements using various different methods [18].

### 3.3 Top quark mass

Recent combined result of the top quark mass measurements by CDF and D0 collaboration in Run I experiment is reported to be 178.0 ± 4.3 GeV [19]. Global EW fits place a 95% CL upper bound on the Higgs mass of ∼260 GeV [20]. The precise measurement of the top quark mass will further constrain the mass bound. The Run II goal of the mass measurement is to control under an uncertainty of 2-3 GeV.

The top mass measurement at CDF largely depends on the fitting techniques to reconstruct the event topology. First, the kinematic equations of the $t\bar{t}$ decay chain are imposed, and then some kinematical variables are fold by the measured quantities out of 16 free parameters in each event. In *lepton+jets* channel, there are 24 configurations for the jets. For each configuration, an event $\chi^2$ is calculated and minimized. The $\chi^2$ takes into account the detector resolution on the measured quantities as well as the W boson and top quark widths. The configuration that yields the minimum $\chi^2$ is taken as the configuration for the event. The distribution of the reconstructed mass is compared and fit to Monte Carlo generated templates with known input top masses.

The CDF has measured the mass of the top quark in *lepton+jets* channel using traditional "template" methods [21], where one mass is reconstructed per event and the resulting mass distribution compared against template distributions from the simulated $t\bar{t}$ events of varying masses. The multivariate templates method [22] is used weighting events according to the probability for the chosen jet-parton assignment to be correct. The Dynamical Likelihood Method [23] uses the probability formed from the $t\bar{t}$ matrix element to utilize maximal information from the events. This method [24] results in the best value of the top quark mass of

$$M_t = 177.8^{+4.5}_{-5.0}(stat.) \pm 6.2(syst.) \quad \text{GeV}.$$

Figure 13 shows the top mass distribution by DLM analysis. The systematic uncertainty is dominated by the measurement of the jet energy.

In *dilepton* channel, due to the presence of two unfold neutrinos, one more extra conditions driven by the Monte Carlo simulation are imposed on the kinematical variables for the neutrinos. The best fit returns

$$M_t = 168.1^{+11.0}_{-9.8}(stat.) \pm 8.6(syst.) \quad \text{GeV},$$

by the neutrino weighting method [25]. The other top mass measurements using *dilepton* channel can be seen in [26].

Summary of the top mass measurement from CDF is presented in Figure 14.

### 3.4 W helicity in top decay

The W boson coming from top decay can be either left-handed (L) or longitudinally (0) polarized. Those fraction for both mixture states is predicted in the Standard Model as

$$f_0 = \frac{\Gamma(t \to bW_0)}{\Gamma(t \to bW_0) + \Gamma(t \to bW_L)} = \frac{M_t^2}{M_t^2 + 2M_W^2} = 0.70,$$

where b-quark mass is neglected and top mass is assumed to be 175 GeV. It is important to check this fraction of the longitudinal component which tells us the symmetry breaking mechanism to give a mass of W boson.

Since the polarization state of the W boson controls the angular distribution of the decaying leptons, CDF has precisely measured the lepton $p_T$ spectra and angular distributions. The estimated $f_0$ value from those distributions constrains to be [27, 28]

$$0.25 < f_0 < 0.88 \qquad \text{at } 95\% \text{ C.L.},$$

which is consistent range of the Standard Model prediction.

### 3.5 Search for single top production

The single top production is linked to the direct measurement of the quark mixing among third generation, $|V_{tb}|^2$, in CKM matrix [29]. The dominant production mechanics are s-channel Drell-Yan production and t-channel associated W boson scattering process. Those production cross sections are proportional to the $|V_{tb}|^2$. If abnormal cross section is observed, it is directory addressed to the coupling with the Wtb electroweak interaction.

However, the single top event has lower jet multiplicities than that of $t\bar{t}$ production events, which suffers significant backgrounds from W + jets events. The optimized search is proposed in [30]. The CDF has searched the single top candidate events, and no candidate observed. We set a limit of [31]

$$\sigma(p\bar{p} \to tb + X) \quad < 17.8 \qquad \text{at } 95\% \text{ C.L.}.$$

## 4 Beyond the Standard Model

### 4.1 Overview

There are several reasons to motivate a new physics beyond the Standard Model: the electroweak symmetry breaking, hierarchy problems, gravitational force, and so forth. Those issues inspire a new theory beyond the Standard Model such as Supersymmetry (SUSY), Grand Unified Theories (GUT), Technicolor (TC), and Extra Dimensions (ED).

These models predict new signatures that can be seen at the experiments with a small production cross section to be compared with the typical QCD events at Tevatron. It is often hard to distinguish new phenomena from the SM background processes. Jet based strategies are overwhelmed by the SM processes, so that the CDF has searched lepton based signatures even through the rates are often suppressed. In this section, a couple of selected studies are only described. Readers may refer [32] for details.

### 4.2 Search for narrow resonance in high mass region

A heavy partner of the Z boson, Z' boson [33], is a by-product predicted by many models of GUT, ED, and little Higgs [34] models. The CDF has searched the excess in high mass Drell-Yan process using *dilepton* events. The invariant mass distribution of *dilepton* events is shown in Figure 15. No excess is found, and limits is set the cross section limits as a function of the spin state since the experimental acceptance changes depending their spin state of the resonance particles. Mass limits for the RPV $\tilde{\nu}$ (spin-0), Z' [37, 38, 34, 39] (spin-1), and RS-graviton [40] (spin-2) are set [35].

The *dijet* events are also used to search for the high mass resonance peak, and limits for some models are set from the cross section limit as shown in Figure 16.

### 4.3 Search for Higgs boson(s)

With high statistic data in Run II, CDF and D0 experiments will start reaching sensitivity to production of low-mass Higgs bosons beyond the limits from LEP experiment. The Standard Model Higgs boson is predominantly decaying into $b\bar{b}$ in the low-mass region. The most promising channel is the associated production with W or Z boson followed by leptonically decay. In high-mass region up to about 180 GeV, Higgs boson produced via gluon fusion might be observable in the decay to WW. In Higgs doublet model, the coupling of the Higgs bosons to b-quarks can be significantly enhanced which allows us to search for the Higgs bosons produced in association with b-quarks. The previous sensitivity studies can be seen in [41, 42].

The CDF has searched the Higgs boson(s), and set the cross section limits as a function of Higgs mass for the searches of the associated production with W boson ($l\nu b\bar{b}$) [43] and Higgs WW decay channel ($l\nu l\nu$ or $l\nu l\nu l\nu$) [44]. The analysis strategies are the same as the top quark measurement in *lepton + jets* channel and the WW cross section measurement. The sensitivity plot is shown in Figure 17. Also, Many other Higgs searches are on-going.

### 4.4 Search for SUSY in *diphoton + missing* $E_T$ channel

Introduction of supersymmetric particles has attractive features for lots of aspects: Higgs self-coupling is converged without fine tuning, all forces except gravity merging in GUT scale, and resulting in many new particles in TeV region, even in cosmology. In this section, a search of Gauge-Mediated SUSY breaking (GMSB) scenario is only described. Many results can be seen in [32].

GMSB can produce a final state of two photons and large missing energy from the lightest supersymmetric particle (LSP), where the lightest neutralino can decay into photon and gravitino (LSP). Thus, *diphoton* candidate events is used in this analysis. The dominant background source is QCD jets events which makes fake missing $E_T$ and photon signals due to the mismeasurement of jets and interaction vertices. After requiring large missing $E_T$ with two identified photons, no candidate is found, and thus set limits [45],

$$m_{\tilde{\chi}_1^\pm} > 93 \text{ GeV} \quad \text{and} \quad \Lambda > 69 \text{ TeV} \qquad \text{at } 95\% \text{ C.L.},$$

where $\Lambda$ is a SUSY-breaking scale. The sensitivity plot is shown in Figure 18.

### 4.5 Search for Leptoquarks

The Leptoquark (LQ) model [46] is natural consequence from GUT theories. The relation between quark and lepton quantum numbers can rule out a triangle anomaly [47], so that the theory is renormalizable. The Leptoquarks are color triplet bosons carrying both lepton and quark quantum numbers, they can be scalar or vector bosons. At Tevatron, they can be pair produced through strong interactions and decay either into a charge lepton and a quark ($\beta = 1$) or a neutrino and a quark ($\beta = 0$).

The CDF has searched two scenarios of $\beta = 1$ and $\beta = 0$ for the scalar type Leptoquarks. Final signatures are $l^+l^-q\bar{q}$ ($\beta = 1$), $\nu\bar{\nu}q\bar{q}$ ($\beta = 0$), and $l\nu q\bar{q}$ ($\beta = 0.5$) for the first and second generations of the scalar Leptoquarks. The results are shown in Figure 19 and 20 in case of $\beta = 1$ and $\beta = 0$, respectively, and limits is set [48]. A search for the third generation Leptoquark is also in progress.

### 4.6 Search for Excited Electron

In the compositeness model for the substructure of quarks and leptons, the excited states of those particles are considerable [49]. The CDF has searched the excited electron, $e^*$, which could be produced through either contact interaction or gauge mediated interactions, and decays into an electron and photon. The signature would be events with $ee\gamma$ with making a mass peak of the excited electron with $M_{e\gamma}$. There is no observation of any deviation from the Standard Model backgrounds. The upper limits are set at 95% C.L. in the parameter space of the excited electron mass and the $M_{e*}/\Lambda$ for the contact interaction model or $f/\lambda$ for the gauge mediated model [50]. Figure 21 and 22 shows the excluded region for the two models, respectively.

# 5 Conclusion

The Tevatron Run II program is in progress since 2001. The CDF experiment have accumulated roughly five times more data than in Run I, with much improved detectors. Many physics results have been produced and more are expected in the near future. Preliminary results on the measurements at CDF are presented, most of all will be published in the near future.

For the electroweak physics, production of weak vector bosons has been measured at a new center of mass energy. The single boson productions have studied, and some fundamental parameters are very precisely driven. The W boson mass will be measured with the accuracy of 25 MeV with a well-established knowledge of the detector. Pairs of gauge bosons are now being produced in reasonably high statistics, and interactions among gauge bosons will be studied in detail.

For the top physics, the top quark measurements have been re-established since Run I experiment, and new measurements just came out in Run II experiment. The top cross section and mass measurements have improved systematics with various analysis techniques. With large data samples, the top mass will be measured with the accuracy of 2 GeV. The studies of the top quark property will push forward with the understandings of top physics.

For new physics searches, many results are improved and marked new limits. In the next a few years, the Tevatron is an unique opportunity to directly search for new physics beyond the Standard Model. The CDF is aggressively looking for new phenomena.

Many other studies not fully covered in this paper are on-going. We hope to see many exciting results from the Tevatron.

# 6 Acknowledgments

The author would like to thank all the people in the CDF Collaboration, and especially Dr. Pasha Murat for the assistance that he provided the information during the Conference. The author would also like to thank the organizers of the Conference.

# References

[1] J. Mariiner, *et al.*, The Tevatron Run II Handbook, See www document, http://www-bd.fnal.gov/lug/runII_handbook/RunII_index.html.

[2] R. Blair, *et al.*, The CDF II Detector Technical Design Report, FERMILAB-Pub-96-390-E, November, 1996.

[3] CDF Collaboration, hep-ex/0406078 (2004), submitted to *Phys. Rev. Lett.*.

[4] P.J. Sutton, *et al.*, Phys. Rev. D **45** (1992) 2349;
P.J. Rijken and W.L. van Neerven, Phys. Rev. D **51** (1995) 44;
R. Hamberg, *et al.*, Nucl. Phys. B **359** (1991) 343;
R.V. Harlander and W.B. Kilgore, Phys. Rev. Lett. **88** (2002) 201801.

[5] K. Hagiwara, *et al.*, Phys. Rev. D **66** (2002) 010001.

[6] CDF Collaboration, http://www-cdf.fnal.gov/physics/ewk/latest_results.html .

[7] CDF Collaboration, FERMILAB-Pub-04-314-E (2004), submitted to *Phys. Rev. D.*

[8] CDF Collaboration, http://www-cdf.fnal.gov/physics/ewk/2004/ww/ .

[9] J.M. Compbell and R.K. Ellis, Phys. Rev. D **60** (1999) 113006;
J. Ellison and J. Wudka, Ann. Rev. Nucl. Part. Sci. **48** (1998) 1.

[10] CDF Collaboration, FERMILAB-Pub-04-246-E (2004), submitted to *Phys. Rev. Lett.*.

[11] U. Baur, *et al.*, Phys. Rev. D **48** (1993) 5140;
U. Baur, *et al.*, Phys. Rev. D **57** (1998) 2823.

[12] F. Abe, *et al.*(CDF Collaboration), Phys. Rev. D **50** (1994) 2966; Phys. Rev. Lett. **74** (1995) 2626;
S. Abachi, *et al.*(D0 Collaboration), Phys. Rev. Lett. **74** (1995) 2632.

[13] D. Acosta, *et al.*(CDF Collaboration), Phys. Rev. Lett. **93** (2004) 142001.

[14] N. Kidonakis and R. Vogt, Phys. Rev. D **68** (2003) 114014.

[15] CDF Collaboration, FERMILAB-Pub-04-275-E (2004), submitted to *Phys. Rev. D.*

[16] CDF Collaboration,
http://www-cdf.fnal.gov/physics/new/top/public/ljets/slt/public_200_files/cdf7174_SLT_200pb-1_public.pdf .
[17] CDF Collaboration,
http://www-cdf.fnal.gov/physics/new/top/confNotes/cdf7154_ttxs_kin_pub.ps .
[18] See CDF Collaboration, http://www-cdf.fnal.gov/physics/new/top/top.html.
[19] The Tevatron Electroweak Working Group, hep-ex/0404010 (2004).
[20] The LEP EW Working Group, http://lepewwg.web.cern.ch/LEPEWWG/
[21] CDF Collaboration, http://www-cdf.fnal.gov/physics/new/top/confNotes/cdf7245_lj_0tag_pub.ps .
[22] CDF Collaboration,
http://www-cdf.fnal.gov/physics/new/top/confNotes/cdf7102_tmass_multivar_-2.ps .
[23] K. Kondo, J. Phys. Soc. Jap. **57** (1988) 4126.
[24] CDF Collaboration,
http://www-cdf.fnal.gov/physics/new/top/confNotes/cdf7056_TopMass_DLM.ps .
[25] CDF Collaboration,
http://www-cdf.fnal.gov/physics/new/top/confNotes/cdf7303_pubTopMass_LTRK_NWA.ps .
[26] See, http://www-cdf.fnal.gov/physics/new/top/confNotes/cdf7194_TopMassDileptonKinemPub.ps ,
http://www-cdf.fnal.gov/physics/new/top/confNotes/cdf7239_dil_template_1.ps .
[27] CDF Collaboration,
http://www-cdf.fnal.gov/physics/new/top/confNotes/cdf7058_top_Whel_pT_public.ps .
[28] CDF Collaboration,
http://www-cdf.fnal.gov/physics/new/top/confNotes/cdf7173_cos_theta_pub_v1_0.ps .
[29] N. Cabbibo, Phys. Rev. Lett. **10** (1961) 531;
M. Kobayashi and T. Maskawa, Prog. Theor. Phys. **49** (1973) 652.
[30] Catalin Ciobanu, *et al.*(CDF Collaboration), Phys. Rev. D **69** (2004) 052003.
[31] CDF Collaboration, FERMILAB-Pub-04-340-E (2004), submitted to *Phys. Rev. Lett.*.
[32] CDF II Exotics Group, http://www-cdf.fnal.gov/physics/exotic/exotic.html .
[33] M. Cvetic and S. Godfrey, hep-ph/9504216 (1995).
[34] T. Han, *et al.*, Phys. Rev. D **67** (2003) 095004.
[35] CDF Collaboration,
http://www-cdf.fnal.gov/physics/exotic/r2a/20040916.dilepton_zprime/note_7286.ps .
[36] D. Choudhury, *et al.*, Nucl. Phys. B **660** (2003) 343.
[37] F. Del Aguila, *et al.*, Nucl. Phys. B **287** (1987) 419.
[38] D. London and J.L. Rosner, Phys. Rev. D **34** (1986) 5.
[39] K.D. Lane and S. Mrenna, Phys. Rev. D **67** (1999) 115011.
[40] L. Randall and R. Sundrum, Phys. Rev. Lett. **83** (1999) 3370.
[41] M. Carena, *et al.*, Report of the Higgs working group of the Tevatron Run II SUSY/Higgs workshop, hep-ph/0010338 (2000).
[42] CDF and D0 Collabration, Results of the Tevatron Higgs Sensitivity Study, FERMILAB-Pub-03-320-E (2003).
[43] CDF Collaboration,
http://www-cdf.fnal.gov/physics/exotic/r2a/20040722.lmetbj_wh_tc/note_7126.ps .
[44] Sunny Chuang (CDF Collaboration), Search for Higgs in WW decays at CDF, presented at PHENO2004, Apr. 26-28, 2004.
[45] CDF Collaboration,
http://www-cdf.fnal.gov/physics/exotic/old.pub_notes/cdf7162_gmsb_ggmet_pub.pdf .
[46] J. Blümlein, *et al.*, Leptoquark Pair Production in Hadronic Interactions, hep-ph/9610408 (1996).
[47] E.A. Kuraev, *et al.*, Sov. J. Nucl. Phys. **51** (1990) 1031;
T.V. Kukhto, *et al.*, Nucl. Phys. B **371** (1992) 567.
[48] CDF Collaboration, FERMILAB-Pub-04-303-E (2004), submitted to *Phys. Rev. Lett.*.
[49] U. Baur, *et al.*, Phys. Rev. D **42** (1990) 815.
[50] CDF Collaboration, FERMILAB-Pub-04-287-E (2004), submitted to *Phys. Rev. Lett.*.

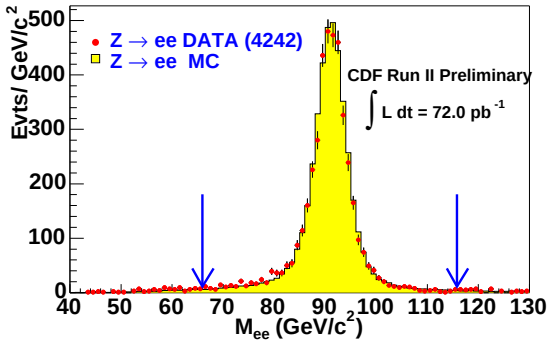


Figure 1: Invariant mass distribution of lepton pairs for $Z \to e^+e^-$ candidates.

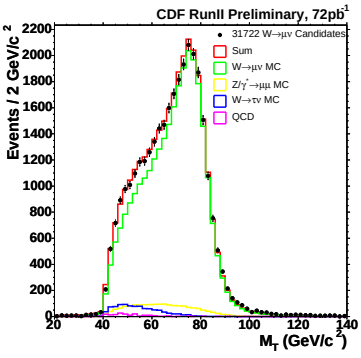


Figure 2: Transverse mass distribution of lepton and missing $E_T$ system for $W \to e\nu$ candidates.

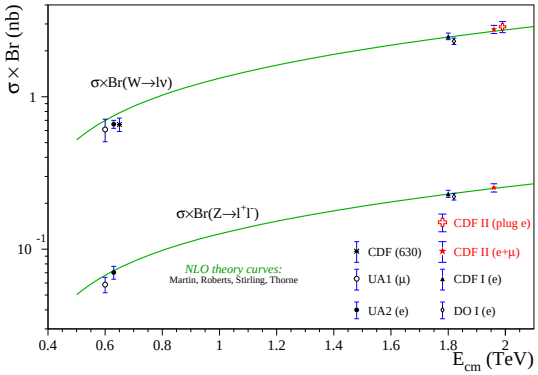


Figure 3: Production cross sections of Z and W bosons as a function of collision center-of-mass energy.

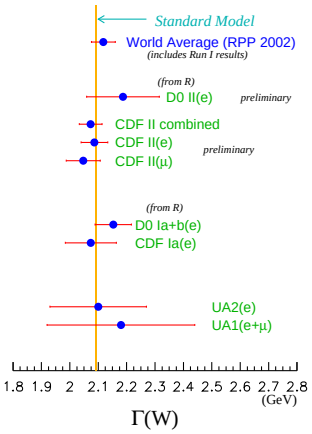


Figure 4: W boson width measurements.

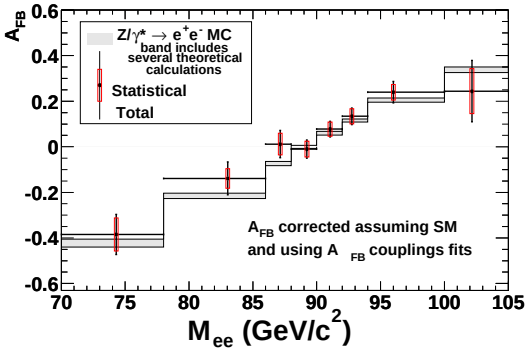


Figure 5: Asymmetry distribution of $Z \to e^+e^-$ events around Z-pole.

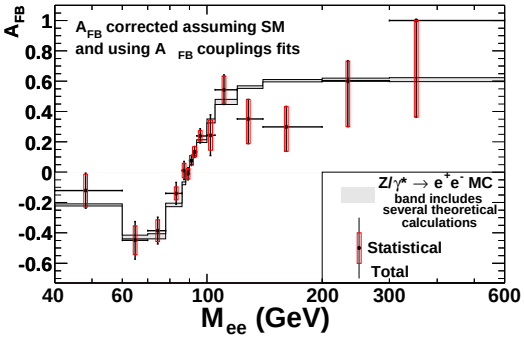


Figure 6: Asymmetry distribution of $Z \to e^+e^-$ events in high mass region.

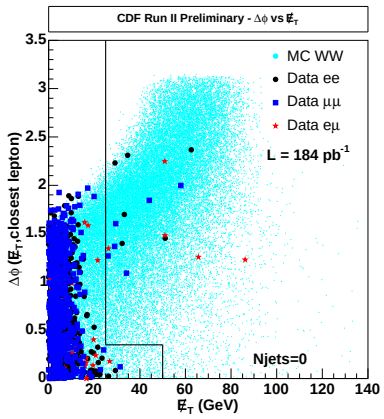


Figure 7: Azimuthal angle between the missing transverse energy and the closest lepton for it.

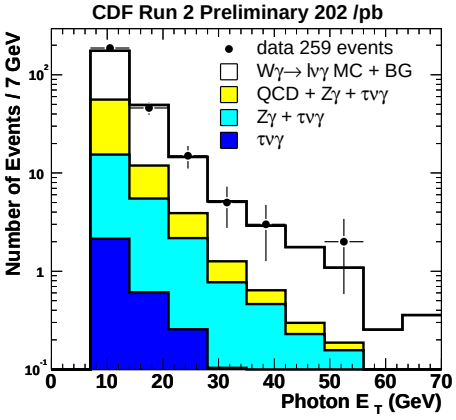


Figure 8: Photon transverse momentum for W$\gamma$ production.

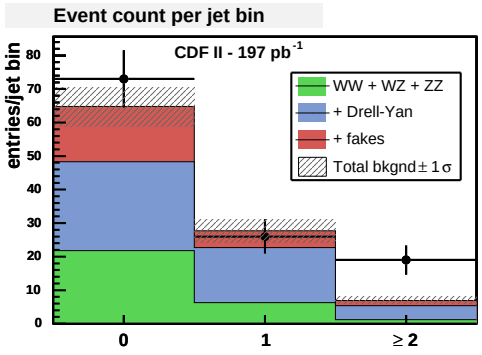


Figure 9: Jet multiplicity distribution of top candidate events in the *dilepton* channel (Lepton+track).

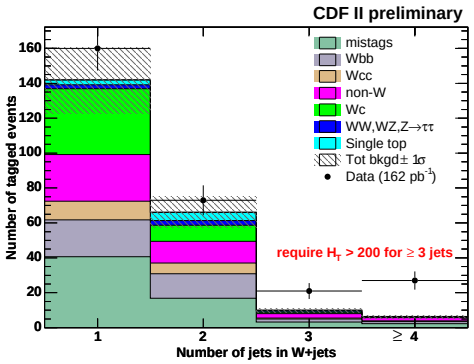


Figure 10: Jet multiplicity distribution of top candidate events in the *lepton+jet* channel with Secondary Vertex b-tagging.

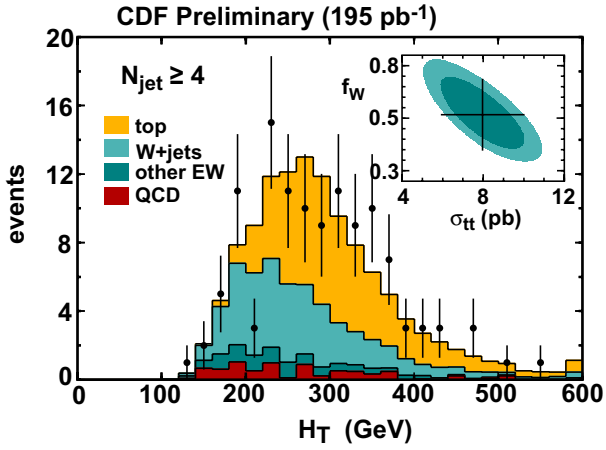


Figure 11: $H_T$ distribution with the expected shapes of signal and backgrounds.

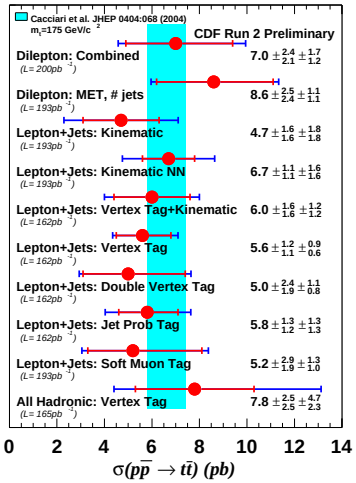


Figure 12: Summary of the measured $t\bar{t}$ cross section from CDF.

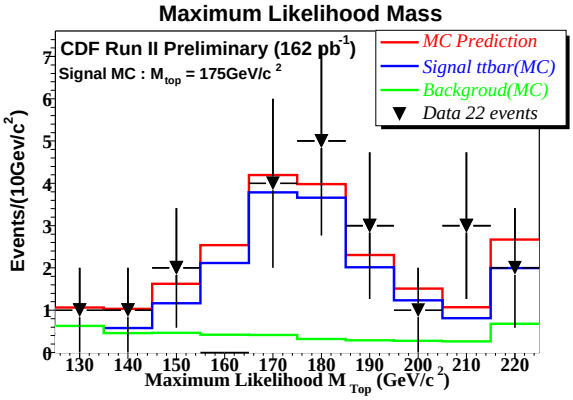


Figure 13: Maximum likelihood mass distribution by DLM analysis.

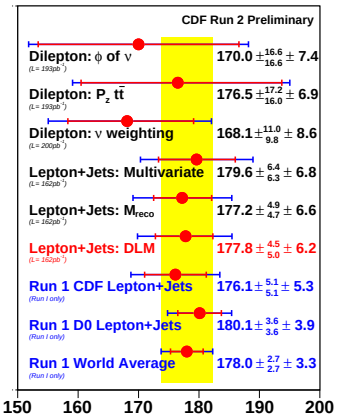


Figure 14: Summary of the measured top mass from CDF.

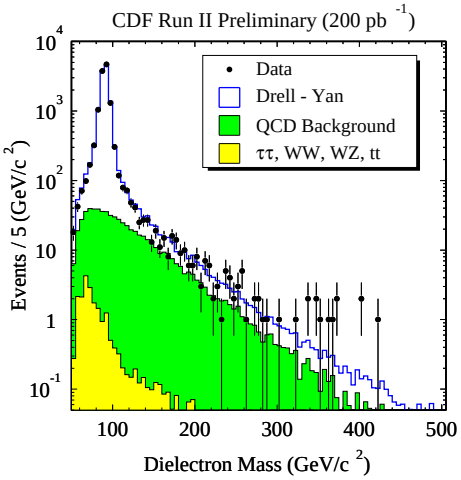


Figure 15: Invariant mass distribution of *dilepton* events.

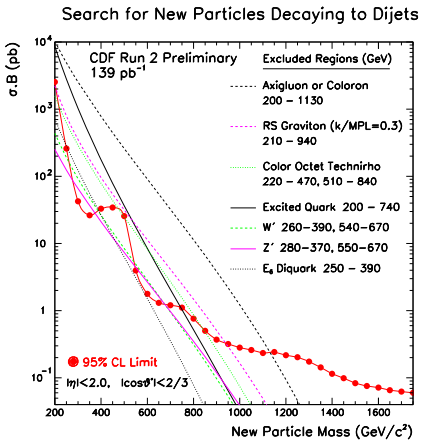


Figure 16: The 95% C.L. upper limit on the cross section times branching ratio for new particles decaying *dijet* for various models.

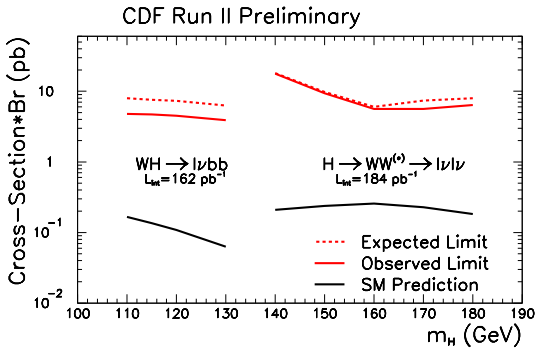


Figure 17: Cross section times branching ratio limit as a function of SM Higgs boson mass.

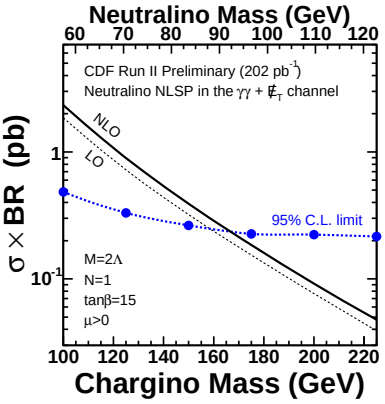


Figure 18: Cross section times branching ratio limit as a function of chargino mass.

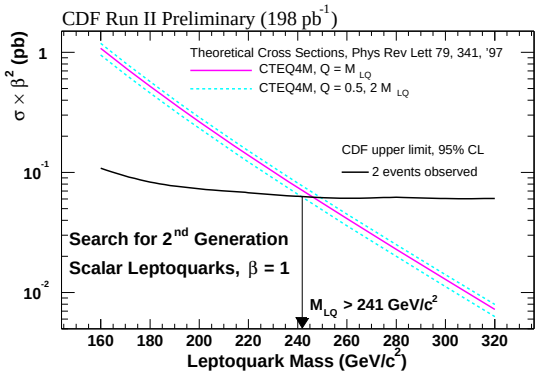


Figure 19: Upper limit on the cross section times squared branching ratio for scalar leptoquark production ($\beta = 1$).

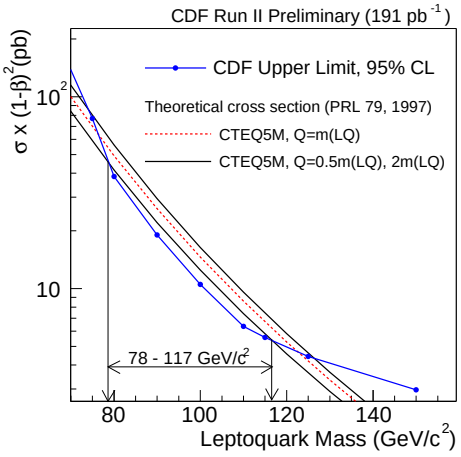


Figure 20: Upper limit on the cross section times squared branching ratio for scalar leptoquark production ($\beta = 0$).

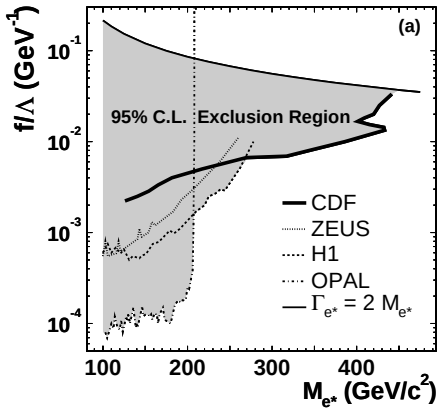


Figure 21: The 95% C.L. excluded region in the parameter space of the gauge-mediated model.

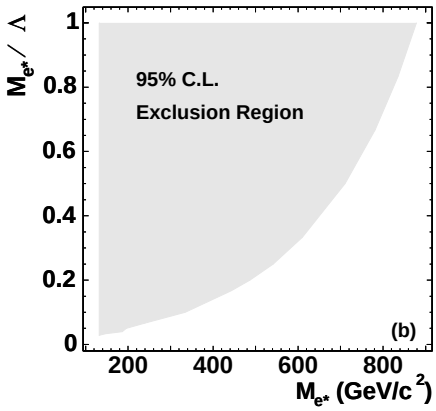


Figure 22: The 95% C.L. excluded region in the parameter space of the contact interaction model.